SF2A 2017
C. Reylé, P. Di Matteo, F. Herpin, É. Lagadec, A. Lançon, Z. Meliani, F. Royer (eds)

FIRST RESULTS FROM THE MAGNETOSPHERIC MULTISCALE MISSION

B. Lavraud[1]

Abstract. Since its launch in March 2015, NASA's Magnetospheric Multiscale mission (MMS) provides a wealth of unprecedented high resolution measurements of space plasma properties and dynamics in the near-Earth environment. MMS was designed in the first place to study the fundamental process of collision-less magnetic reconnection. The two first results reviewed here pertain to this topic and highlight how the extremely high resolution MMS data (electrons, in particular, with full three dimensional measurements at 30 ms in burst mode) have permitted to tackle electron dynamics in unprecedented details. The first result demonstrates how electrons become demagnetized and scattered near the magnetic reconnection X line as a result of increased magnetic field curvature, together with a decrease in its magnitude. The second result demonstrates that electrons form crescent-shaped, agyrotropic distribution functions very near the X line, suggestive of the existence of a perpendicular current aligned with the local electric field and consistent with the energy conversion expected in magnetic reconnection (such that $\mathbf{J} \cdot \mathbf{E} > 0$). Aside from magnetic reconnection, we show how MMS contributes to topics such as wave properties and their interaction with particles. Thanks again to extremely high resolution measurements, the lossless and periodical energy exchange between wave electromagnetic fields and particles, as expected in the case of kinetic Alfvén waves, was confirmed. Although not discussed, MMS has the potential to solve many other outstanding issues in collision-less plasma physics, for example regarding shock or turbulence acceleration, with obvious broader impacts in astrophysics in general.

Keywords: collision-less magnetic reconnection,kinetic Alfvén waves, electron stochastic dynamics

1 Introduction

With the advent of the space era, it has become possible to study astrophysical plasma processes in situ. Although the plasma regime (density, temperature, magnetic field magnitude) in near-Earth space is not necessarily comparable to those in more remote astrophysical objects such as active galactic nuclei or just the Sun, it remains that near-Earth space is the only accessible astrophysical plasma from which we can hope to extrapolate our knowledge to more exotic environments. From already several decades of in situ space measurements we have increased our understanding of many key plasma processes, such as magnetic reconnection, shocks, wave-particle interactions and turbulence, among others. The Earth's magnetosphere, depicted in Figure 1, constitutes for that purpose a perfect natural laboratory. The interaction between the solar wind and the magnetosphere indeed results in the formation of various regions and boundaries where these fundamental processes are at work. The first interaction with the solar wind occurs at the fast mode wave shock, which slows down, heats and deflects the solar wind plasma along the magnetospheric flanks in a region known as the magnetosheath. This often turbulent medium is the region in direct contact with the magnetosphere at the magnetopause. The magnetopause is thus the location where plasma and energy transfer between the solar wind and the magnetosphere occurs, and magnetic reconnection is the key process at work in that respect. The process of magnetic reconnection is ubiquitous in the plasma universe. Although it has major large-scale implications on the surrounding media, the processes that control magnetic reconnection occur at very small scales in a region known as the diffusion region (where magnetic fields diffuse and reconnect with a new topology) (e.g., Priest & Forbes 2000). In proton-electron plasmas, as observed near-Earth for instance, the vastly different particle masses lead to a structured region wherein the ions (with larger gyro-radius) decouple from the magnetic field farther from the X-line (where the topology changes) than electrons. This separation leads

[1] Institut de Recherche en Astrophysique et Planétologie, Université de Toulouse, France

to the formation of an ion diffusion region with characteristic Hall currents and magnetic fields embedding a much smaller electron diffusion region (e.g., Øieroset et al. 2001; Mozer et al. 2002). While missions such as the multi-spacecraft Cluster mission have instrumentation and inter-spacecraft separation on the order of the typical ion scales at the Earth's magnetopause, the Magnetospheric Multiscale (MMS) mission has been designed to understand the electron-scale physics associated with magnetic reconnection (Burch et al. 2015). In this paper we highlight a few selected MMS results that pertain to particle dynamics, and their interaction with waves, at spatio-temporal scales that were way beyond reach before the MMS era.

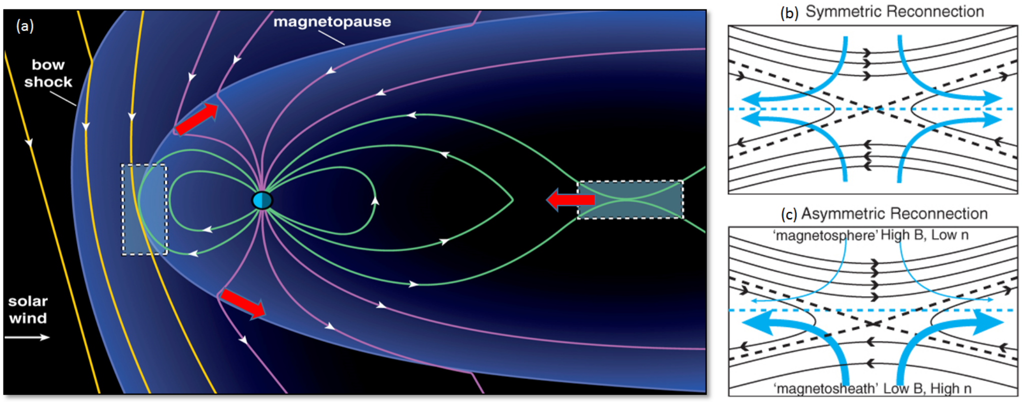

Fig. 1. (a) Schematic of the Earth's magnetosphere with its main surrounding boundaries. Two rectangles are highlighted where magnetic reconnection is known to occur; at the dayside magnetopause and in the magnetotail. The main flow patterns resulting from reconnection, and driving magnetospheric convection in the magnetosphere, are shown with red arrows. (b) Schematic of the magnetic reconnection topology and flows for symmetric plasma properties on each side of the X line. (c) Similar to (b) but for asymmetric plasma properties. Adapted from Eastwood et al. (2013).

2 The MMS mission

The four NASA MMS (Burch et al. 2015) spacecraft were launched together on March 12, 2015 on an Atlas V launch vehicle into a highly elliptical 28°-inclination orbit with perigee at 1.2 Earth radii (RE) and apogee at 12 RE. The results reviewed here are based on ion and electron measurements from the Fast Plasma Instruments (FPI, Pollock et al. 2016)), magnetic field measurements from the FluxGate Magnetometers (FGM, Russell et al. 2016)), and electric field data from the Electric Double Probe instrument, which consists of the Spin Plane Double Probe (SDP, Lindqvist et al. 2016)) and the Axial Double Probe (ADP, Ergun et al. 2016)). With a 12 RE apogee, the first 2 years of the MMS mission were dedicated to the study of magnetic reconnection at the dayside magnetopause (Figure 1a, left rectangle). Magnetic reconnection there takes place between two plasmas with very different properties (density, temperature and magnetic field in particular); magnetic reconnection is said to be asymmetric (cf. Figure 1c). After 2 years, the apogee of the MMS spacecraft has recently been increased to 25 RE so as to focus on the process of magnetic reconnection in the magnetotail (right-hand side rectangle in Figure 1c). In the magnetotail, reconnection occurs between the south and north lobe regions, which have very similar properties; magnetic reconnection is said to be symmetric. In addition to a smart orbit design, permitting to sample various types of reconnection properties, the main requirements for meeting the MMS mission objectives were: (1) four spacecraft in a close tetrahedron formation with adjustable separations down to less than 10 km, (2) accurate three-axis electric and magnetic field measurements for estimating spatial gradients and time variations, and (3) three-dimensional electron and ion distribution functions at the highest time resolution ever achieved (30 ms for electrons and 150 ms for ions). Requirement (1) is particularly critical to discriminate spatial from temporal variations in in situ measurements. Indeed, with a single spacecraft it is essentially impossible to determine if a signature in the time series is due to a spatial structure passing by the spacecraft (e.g., back and forth motion of a boundary) or the result of a temporal variation (e.g., a propagating wave). Requirement (2) stems from the fact that the calculation of gradients, e.g. the electric current using Ampère's law in the Curlometer technique (Robert et al. 1998), across the tetrahedron at such small scales requires high fidelity electromagnetic field measurements to limit the propagation of errors (in the gradient method). Then, a major leap forward brought by MMS is the unprecedentedly high temporal resolution of full three-dimensional particle measurements. It is a factor 100 higher than past measurements for electrons, consistent with the requirement (3) to study electron dynamics at the electron scale.

3 Electron dynamics in highly curved magnetic fields

Among all MMS first amazing results, many have come from its 30 ms electron measurements, which permit the study of electron dynamics in unprecedented details. Electron dynamics in collisionless magnetic reconnection has been studied mostly using test particle (Speiser 1965) and particle-in-cell (PIC) simulations (e.g., Hoshino et al. 2001; Hesse et al. 2014). For the present topic, of particular interest is the prediction that particle pitch angle scattering should occur when the gyroradius of a particle is on the order of the scale of the local magnetic field curvature. With RC the local magnetic field curvature and RG the particle gyroradius, one can define an adiabatic parameter κ such that $\kappa^2 = RG/RC$. Based on this parameter, theory predicts that particle scattering (of ions or electrons) occurs when κ^2 approaches 25, and that particle dynamics becomes chaotic for values below 10 (Büchner & Zelenyi 1989; Sergeev et al. 1983). Although there have been a few observations of non-adiabatic proton and electron dynamics in the tail region of the Earth for high energy particles (Egedal et al. 2005; Shen et al. 2014), only theory and numerical modeling were so far able to study the complex behavior of thermal electrons at electron scales (Ng et al. 2011; Hesse et al. 2014; Wang et al. 2016). No appropriate spacecraft observations were available before MMS. Such small-scale electron dynamics is illustrated in Figure 2. This Figure shows a typical anti-parallel magnetic reconnection geometry with reconnecting field lines in purple and an example electron trajectory in black. The underlying red and blue colors represent the out-of-plane magnetic field (generally called the Hall magnetic field). A spacecraft trajectory is shown with a red arrow. It is taken as representative of the crossing of a reconnecting magnetopause that occurred on 16 October 2015 (shown in Figure 2b). Apart from the magnetic field lines and spacecraft trajectory (both drawn for context) the Hall field and electron trajectory are direct outputs from a kinetic simulation made by Bessho et al. (2015). The key signature to note in Figure 2a is the non-adiabatic electron behavior. Indeed, as the example electron moves from point 1 to point 2 toward the X line, the magnetic field magnitude decreases significantly (not shown). In addition, as a result of reconnection a strong current sheet is formed along points 2 to 7 where the Hall magnetic field switches sign. The magnetic field is thus lower but also highly curved all along this current sheet. This combination of low and curved magnetic field leads to a non-adiabatic behavior such that when the electron reaches point 2 it is scattered back toward the same side of the current sheet. Had the electron behaved adiabatically, it would have crossed towards the other side of the current sheet. The same behavior is observed at points 4 and 5, while the electron traverses the current sheet at points 3, 6 and 7. Figure 2b shows data from MMS spacecraft # 4 on 16 October 2015 during a crossing of the dayside magnetopause. The spacecraft are traversing from the magnetosphere (to the left) to the magnetosheath (to the right). Although not shown, all plasma parameters are consistent with such a crossing (cf. Lavraud et al. 2016). We only focus here on the pitch angle distribution (i.e., the angle between the velocity of the electron and the magnetic field direction) of 100 eV electrons in the upper panel, and on the magnetic field curvature in the second panel. The magnetic field radius of curvature (RC) is measured thanks to a four-spacecraft gradient method, as described in more detail in Shen et al. (2003). On the magnetospheric side of the magnetopause (to the left) electrons are strongly magnetized, as demonstrated by the strong anisotropy with much larger fluxes in the field-aligned (0°) and anti-field-aligned (180°) directions. Similarly, electrons are fully magnetized in the magnetosheath (right-hand side), with a highly structured pitch angle distribution. By contrast, electrons are very isotropic in the center of the region, close to the location where the magnetic field is most curved. Together with some other signatures, not detailed here, these observations are consistent with the scattering observed in the simulation of Figure 2a. These are the first observations of thermal electron pitch-angle diffusion associated with magnetic reconnection.

4 Currents and crescent electron distributions

Another major, recent observation is that of crescent electron distribution functions (Burch et al. 2016) in the electron diffusion region of magnetic reconnection. This naming comes from the representation shown in Figure 3a. It shows a cut of the three-dimensional distribution function of electrons in the plane perpendicular to the magnetic field. The distribution function shown corresponds to a time when it is believed that the spacecraft crossed the electron diffusion region of magnetic reconnection very close to the X line of the dayside magnetopause (also on 16 October 2015, but at a time different from the event of Figure 2). This highly non-gyrotropic (i.e., not axially symmetric in the plane perpendicular to the magnetic field) distribution carries a

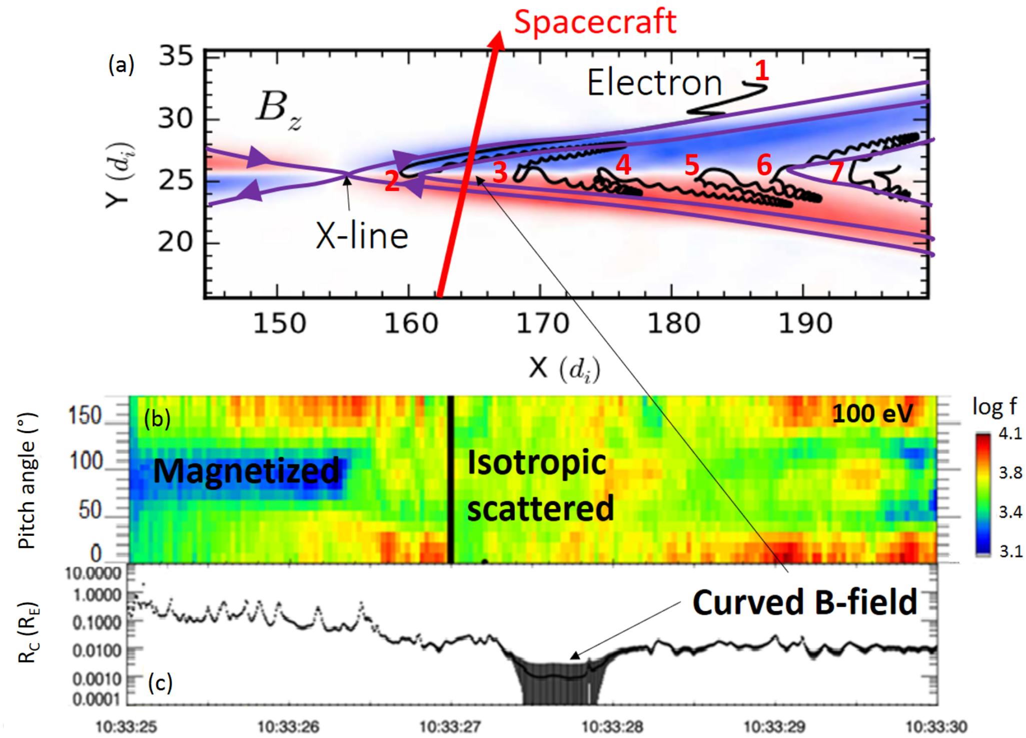

Fig. 2. (a) Illustration of an electron trajectory (black line) in the magnetic field geometry (purples lines) near a magnetic reconnection X line. Red and blue colors show the out-of-plane (Hall) magnetic field component. Seven specific locations of the electron trajectory are marked with red numbers. These are further discussed in the text. We also illustrate the rough trajectory of the MMS spacecraft that is consistent with the observations shown in panels (b) and (c). Panel (a) is adapted from a simulation by Bessho et al. (2015). Panels (b) and (c) are adapted from Lavraud et al. (2016). They show, respectively, (b) the pitch angle distribution of 100 eV electrons as a function of time during a crossing of the MMS spacecraft near an X line, together with (b) the magnetic field radius of curvature as estimated using a multi-spacecraft technique Shen et al. (2003) during the same interval. The time at which electrons become isotropic is shown with a vertical line in panel (b).

strong perpendicular current. This perpendicular current has the same orientation as the local electric field $\mathbf{E}$ (as measured by the EDP instrument) so that $\mathbf{J} \cdot \mathbf{E}$ is positive as observed in Figure 2b ($\mathbf{J}$ is the current density vector). It should be noted that this signature is confirmed by the independent calculations of the current based on the multi-spacecraft curlometer method and the direct particle measurements, i.e., $\mathbf{J} = Nq(\mathbf{V_i} - \mathbf{V_e})$ (where N is the plasma density, q the electric charge, and $\mathbf{V_i}$ and $\mathbf{V_e}$ respectively the ion and electron velocity vectors). Such direct current estimations using ion and electron data (velocity and density) had never been achieved before the high resolution, high accuracy MMS measurements. The interpretation is that such crescent electron distributions appear exactly at the X line as a result of Speiser-type (Speiser 1965) meandering electron orbits in the local inversion of the magnetic field, and that the resulting current is consistent with that expected from a dissipative process such as magnetic reconnection (with $\mathbf{J} \cdot \mathbf{E} > 0$).

5 Electromagnetic field and particles interaction in kinetic Alfvén waves

Although MMS was specifically tailored for the study of magnetic reconnection, the mission is able to tackle many other plasma physics questions. Among these is the exact mechanics of waves and wave-particle interactions. The Alfvén wave is the most ubiquitous wave mode in plasma physics (Alfvén 1942). When the wavelength is large compared to the thermal ion scale, no energy is transferred between the field and the plasma. However, when the wave's perpendicular spatial scale approaches this scale, the Alfvén wave propagates obliquely and can support a significant parallel electric field. This property means the existence of a transfer of energy between the wave and the particles (Hasegawa & Chen 1976). Such kinetic Alfvén waves (KAW) are of critical importance both in laboratory (e.g., Wong 1999) and space environments (e.g., Louarn et al. 1994). Thanks

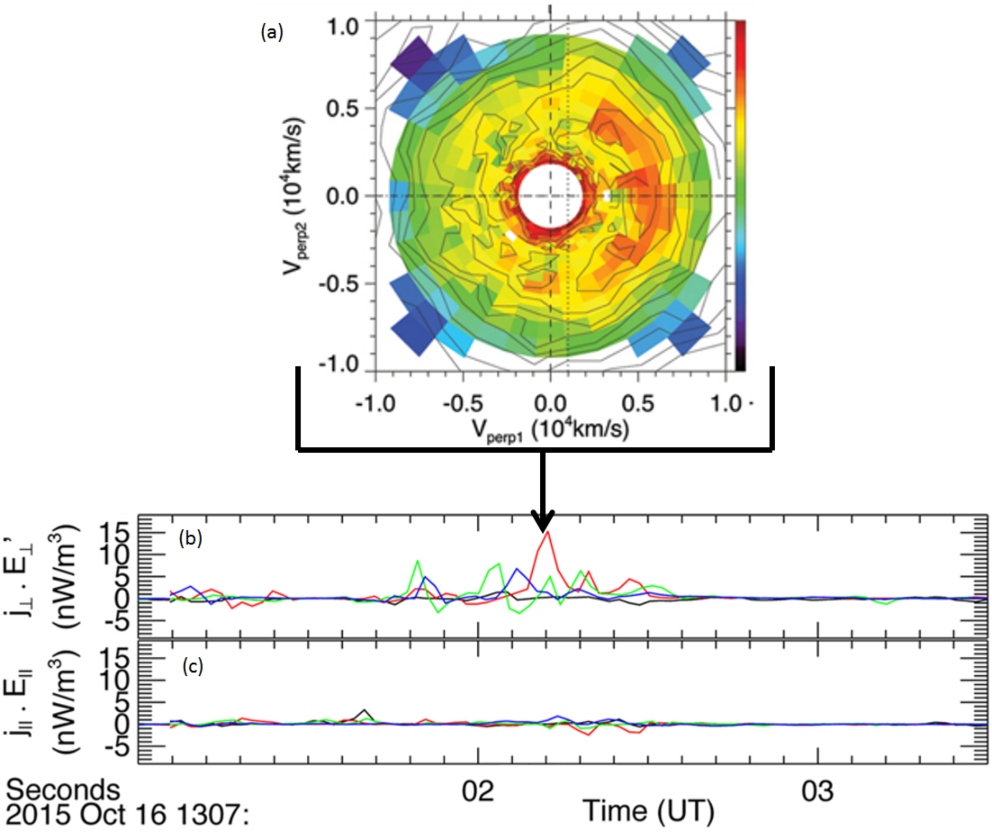

Fig. 3. (a) Cut of a three-dimension electron distribution function in the plane perpendicular to the local magnetic field during an X line crossing (electron diffusion region) on 16 October 2015. The color coding shows the phase space density of electrons. (b) Perpendicular and (c) parallel components of $\mathbf{J} \cdot \mathbf{E}$, the plasma heating term. Adapted from Burch et al. (2016).

to high resolution MMS data in the Earth's magnetosphere, Gershman et al. (2017) recently demonstrated the direct exchange of energy between plasma particles and fields in a marginally stable KAW train.

The current ($\mathbf{J}$) and electron-pressure-gradient-driven electric field ($\mathbf{Ep} = -\nabla \cdot \mathbf{Pe}/(nee)$) are perpendicular to each other in regular Alfvén wave fluctuations. $\mathbf{J} \cdot \mathbf{E}$, the plasma heating term, is thus equal to zero throughout the entire wave. Gershman et al. (2017) recently studied MMS observations of low frequency ($\sim$ 1 Hz) fluctuations akin to a KAW train in the dayside magnetosphere close to the magnetopause. The observations showed that the perpendicular and parallel components of $\mathbf{J}$ and $\mathbf{Ep}$ were $\sim 90°$ out-of-phase with respect to each other, as shown in Figure 4. This phase difference implies a non-zero value of $\mathbf{J} \cdot \mathbf{E}$ throughout the wave train, thereby demonstrating for the first time the instantaneous and very local nature of energy exchange between electromagnetic fields and particles within KAW.

Although not shown, Gershman et al. (2017) also uncovered an unpredicted population of electrons trapped within the wave fluctuations. The unprecedented high resolution measurements by the MMS spacecraft thus also open the door to a whole new unexplored territory in wave-particle interaction physics.

6 Conclusions

We have reviewed a few chosen results from NASA's recent Magnetospheric Multiscale (MMS) mission. Thanks to its unprecedented high-resolution measurements, the intricate dynamics of electron populations and associated currents in the vicinity of the diffusion region of magnetic reconnection at Earth's dayside magnetopause are revealed. This review only mentions three results: (1) the demagnetization and scattering of electrons at very small scales (and energies) owing to highly curved magnetic field lines, (2) the formation of crescent-shaped electron distribution functions at the X line, and whose perpendicular current is consistent with the conversion of magnetic energy into particle energy ($\mathbf{J} \cdot \mathbf{E} > 0$), and (3) the lossless and periodical energy exchange between

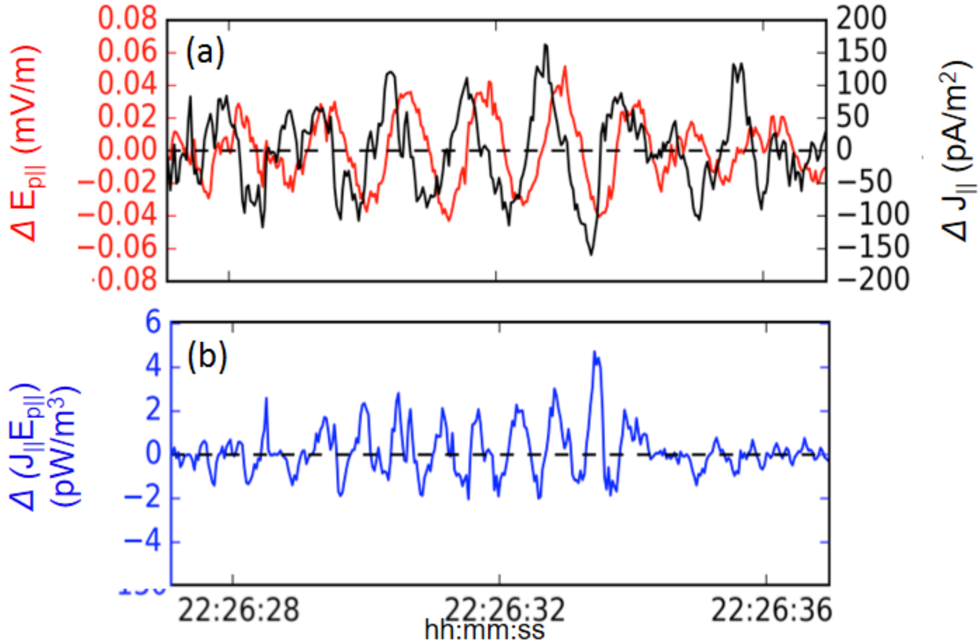

Fig. 4. (a) Parallel components of the current ($\mathbf{J}$) and electron-pressure-gradient-driven electric field ($\mathbf{E_p}$) during a kinetic Alfvén wave fluctuation. Panel (b) shows the non-zero variations of $\mathbf{J}_{\|} \cdot \mathbf{E}_{\mathbf{p},\|}$, the plasma heating term, which demonstrates the direct exchange of energy between plasma particles and fields in this KAW train. Adapted from Gershman et al. (2017).

electromagnetic fields and particles in kinetic Alfvén waves. There are already many other results compiled, for instance, in two special sections of Geophysical Research Letters and Journal of Geophysical Research, in 2016 and 2017, respectively. The topics addressed also involve shocks and turbulence, two domains in which MMS will undoubtedly shed important new lights in the coming years.

For MMS data visit `https://lasp.colorado.edu/mms/sdc/public/`. We thank all the MMS teams for their remarkable work and great hardware accomplishments. Work at IRAP and LPP was performed with the support of CNRS and CNES.

References

Alfvén, H. 1942, Nature, 150, 405

Bessho, N., Chen, L.-J., Germaschewski, K., & Bhattacharjee, A. 2015, Journal of Geophysical Research (Space Physics), 120, 9355

Büchner, J. & Zelenyi, L. M. 1989, in Proceedings of an international Workshop on Reconnection in Space Plasma, ed. C. I. Meng, M. J. Rycroft, & L. A. Frank, Vol. 2, Europen Space Agency, Paris, 21

Burch, J. L., Moore, T. E., Torbert, R. B., & Giles, B. L. 2015, Space Sci. Rev.

Burch, J. L., Torbert, R. B., Phan, T. D., et al. 2016, Science

Eastwood, J. P., Phan, T. D., Drake, J. F., et al. 2013, Physical Review Letters, 110, 225001

Egedal, J., Øieroset, M., Fox, W., & Lin, R. P. 2005, Physical Review Letters, 94, 025006

Ergun, R. E., Tucker, S., Westfall, J., et al. 2016, Space Sci. Rev., 199, 167

Gershman, D. J., F-Viñas, A., Dorelli, J. C., et al. 2017, Nature Communications, 8, 14719

Hasegawa, A. & Chen, L. 1976, Physical Review Letters, 36, 1362

Hesse, M., Aunai, N., Sibeck, D., & Birn, J. 2014, Geophys. Res. Lett., 41, 8673

Hoshino, M., Mukai, T., Terasawa, T., & Shinohara, I. 2001, J. Geophys. Res., 106, 25979

Lavraud, B., Zhang, Y. C., Vernisse, Y., et al. 2016, Geophys. Res. Lett., this issue

Lindqvist, P.-A., Olsson, G., Torbert, R. B., et al. 2016, Space Sci. Rev., 199, 137

Louarn, P., Wahlund, J. E., Chust, T., et al. 1994, Geophys. Res. Lett., 21, 1847

Mozer, F. S., Bale, S. D., & Phan, T. D. 2002, Physical Review Letters, 89, 015002

Ng, J., Egedal, J., Le, A., Daughton, W., & Chen, L.-J. 2011, Physical Review Letters, 106, 065002

Øieroset, M., Phan, T. D., Fujimoto, M., Lin, R. P., & Lepping, R. P. 2001, Nature, 412, 414

Pollock, C., Moore, T., Jacques, A., et al. 2016, Space Science Rev., 199, 331

Priest, E. & Forbes, T., eds. 2000, Magnetic reconnection : MHD theory and applications

Robert, P., Dunlop, M., Roux, A., & Chanteur, G. 1998, in Analysis Methods for Multi-Spacecraft Data, ed. G. Paschman & P. Daly, ISSI Scientific Report SR-001 (European Space Agency), 395–418

Russell, C. T., Anderson, B. J., Baumjohann, W., et al. 2016, Space Sci. Rev., 199, 189

Sergeev, V. A., Sazhina, E. M., Tsyganenko, N. A., Lundblad, J. A., & Soraas, F. 1983, Planet. Space Sci., 31, 1147

Shen, C., Li, X., Dunlop, M., et al. 2003, Journal of Geophysical Research (Space Physics), 108, 1168

Shen, C., Yang, Y. Y., Rong, Z. J., et al. 2014, Journal of Geophysical Research (Space Physics), 119, 2458

Speiser, T.-W. 1965, J. Geophys. Res., 70, 4219

Wang, S., Chen, L.-J., Bessho, N., et al. 2016, Journal of Geophysical Research (Space Physics), 121, 2104

Wong, K.-L. 1999, Plasma Physics and Controlled Fusion, 41, R1